Evaluating the effectiveness of Red Onion Skin Extract Derivatives as oilfield scale inhibitors

ABSTRACT

With growing awareness of the environmental impact of some conventional production chemicals and concerns about the depletion of non-renewable natural resources, increased efforts are being made to use renewable and non-toxic materials in the oilfield. In this study, a potential green scale inhibitor was developed from the skin of red onions and evaluated for calcium sulphate, calcium carbonate and barium scale inhibition. Based on the different extraction processes utilized, two products were obtained and characterized using FTIR and SEM and evaluated using a static jar test procedure. The FTIR results confirmed the bands that make up the major constituents (quercetin) and other important compounds, which supports the present study. Laboratory evaluation show that ROSE can efficiently inhibit calcium sulphate scale and barium sulphate scales with a good inhibition rate of greater than 75 % at an optimum dosage. Effect of temperature and dosage on inhibition performance revealed that ROSE is stable at higher temperatures and can effectively inhibit calcium and barium sulphate scales at nearly the same rate without degradation but requires additional dosage to produce same result for calcium carbonate scale. Also, the effect of time reveals that scale inhibitor performs a continuous $CaSO_4$ and $CaCO_3$ inhibition. Not only does ROSE perform excellently in the laboratory condition as a green scale inhibitor, but it also show a relatively close performance rate when compared to an existing commercial inhibitor which indicate that ROSE has a high potential for use in the oil industry.

Keywords: *calcium sulphate scale; calcium carbonate scale; barium sulphate scale; red onion skin; green scale inhibitor; scale inhibition.*

Glossary: *ROSE – Red Onion Skin Extracts; FTIR- Fourier transform infrared spectroscopy; NaOH-Sodium hydroxide; SEM - Scanning Electron Microscope,* $CaSO_4$ *– Calcium sulphate;* $CaCO_3$ *– Calcium carbonate;* $BaSO_4$ *– Barium sulphate;* $SrSO_4$ *- strontium sulfate. NaCl - Sodium chloride;* $CaCl_2 \cdot 2H_2O$ *- Calcium*

Chloride, Dihydrate; $MgCl_2$•$6H_2O$ - Magnesium chloride hexahydrate; Na_2SO_4-Sodium sulfate; $BaCl_2$•$2H_2O$ - Barium chloride, dihydrate.

1. Introduction

Scale inhibitor is a term generally used to describe a class of chemicals used to mitigate the formation or deposition of scale. Scale is an inorganic precipitation formed on metal or rock surfaces, wellbore tubulars and other wellbore equipment [1-2]. Scale inhibition can occur when one or more aspects of the crystallization process is disrupted [2-3]. Sulfate and carbonate scales have been identified as the most common inorganic scales found in oilfields worldwide [4-6] While Sulfate scales, which include calcium sulfate ($CaSO_4$), barium sulfate ($BaSO_4$) and strontium sulfate ($SrSO_4$) are formed due to the mixing of incompatible brines, specifically formation brine and injected seawater, carbonate scales are deposited due to change in operating conditions, such as drop in pressure in production wells [4-5, 7-8]. Mineral scale formation can be described with the following reactions [3].

$$Ca^{2+}_{(aq)} + 2HCO^{3-}_{(aq)} \rightarrow CaCO_{3\,(s)} + CO_2 + H_2O$$
$$Ca^{2+}_{(aq)} + SO_4{}^{2-}_{(aq)} \rightarrow CaSO_{4\,(s)}$$
$$Ba^{2+}_{(aq)} + SO_4{}^{2-}_{(aq)} \rightarrow BaSO_{4\,(s)}$$

To mitigate the problem of mineral scaling, chemical inhibitors are widely used. However, some of these chemical inhibitors are toxic and environmentally unsafe for application. With the increasing awareness of environmental impact caused by hazardous production chemicals, efforts have been made to utilize green scale inhibitors. Recently, green inhibitors, have raised great interest because they are biodegradable, non-toxic and do not affect environment non-bioaccumulation [9-11].

Quercetin, as shown in Figure 1a has been discovered to have good inhibiting effect due to its high antioxidative and excellent metal chelation properties like other flavonoids [12-18]. The metal chelating property is attributed to the presence of five (5) hydroxyl groups at positions 3,3',4'5,7, and a carbonyl group at position 4 as shown in Figure 1b [3]. Red onion skin (ROS) contains the highest concentration of "quercetin" [19-20] and other polyphenolic compounds [21-22] which can easily be extracted and used in the oil industry. However, "onion skins" are usually discarded as wastes which becomes a nuisance to the environment especially when they are disposed improperly the discovery of this active ingredient in red

onion skin prompted this investigation to harness the properties of quercetin as a potential green scale inhibitor.

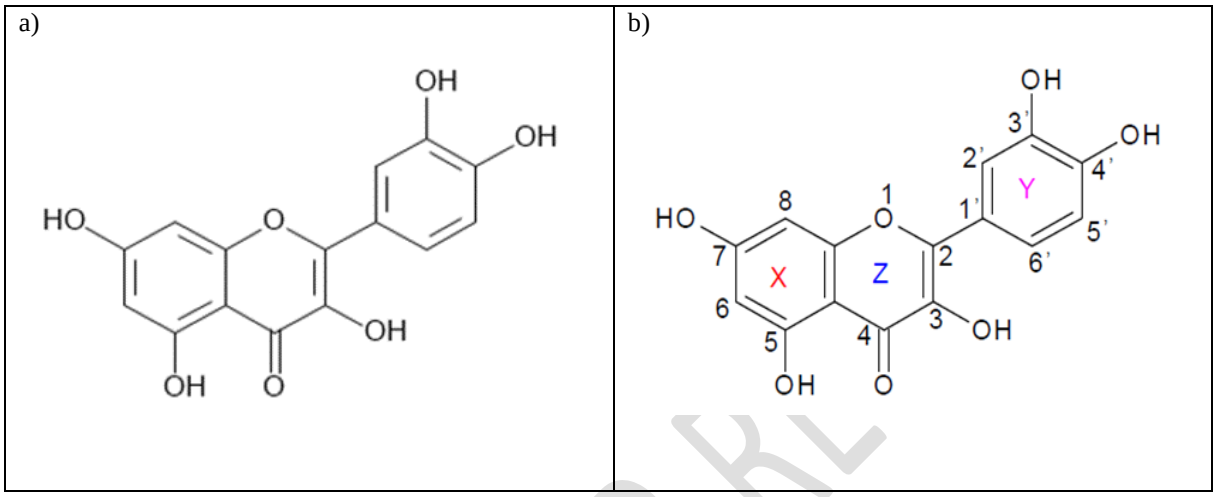

Figure 1: (a) Structure of Quercetin, (b) Functional group positions of Quercetin [3]

2. Materials and Methods

2.1. Collection and pretreatment of ROS

Discarded onion skins from processed onions were collected from markets in Port Harcourt, Rivers State, Nigeria. They were carefully selected and thoroughly washed with distilled water to remove impurities. Thereafter, air dried at ambient temperature and pulverized into powder form using a fabricated grinder and then stored in airtight plastic containers for further use.

2.2. Extraction process

This study adopted two extraction processes: a solvent extraction mechanism [3, 23] and cold extraction process [24].

2.2.1 Solvent extraction method

Solvent extraction mechanism involves the use of a low boiling point liquid to get out extract from materials. The choice of this technique is its ability to extract up to 99.5 % of the extract from its bearing material,

leaving 0.5 % as a residual [25]. In this study, Soxhlet extractor apparatus was used while acetone served as the extracting solvent.

2.2.3 Cold Extraction method

The second extraction method involved soaking clean red onion skin in 1 percent NaOH for 24 hours. After that, the soluble extracts were filtered. To separate red onion skin extract from water, a rotary evaporator was used. Thereafter, the extract was air dried for approximately 30 days to allow any remaining moisture to evaporate.

2.3. Characterization of Scale Inhibitor and deposited scale crystal

Fourier transform infrared spectroscopy, FTIR (Agilent Cary 630, US in transmission mode from 4000 to 600 cm^{-1}) was used to determine the presence of various functional groups in the proposed scale inhibitors. Further investigation to assess the morphology of the scale deposition with and without inhibitor was carried out using Scanning electron microscope, SEM (HITACHI S-4800, Japan). Calcium sulphate, calcium carbonate, barium sulfate, depositions were carefully sampled at low/no inhibitor dosage.

2.4. Evaluation of the inhibition efficiency

To evaluate the inhibition efficiency, a static jar test was done using National Association of Corrosion Engineers (NACE) Standard TM0374-2007 procedures [26, 27]. Table 1 shows the solutions prepared for evaluating the scale inhibition performance. After weighing a specific amount of scale inhibitor (20 ppm, 40 ppm, 60 ppm, 80 ppm and 100 ppm) into the Erlenmeyer flask, 50 mL of cation solution (as specified in NACE standard) was added and agitated for proper mixing, followed by another 50 mL of anion solution. The test bottle was sealed with a plastic stopper and wrapped in polyethylene film. The wrapped Erlenmeyer flasks were placed in the oven for a predetermined time at a constant temperature. The inhibitor efficiency was calculated based on the remaining $Ca^{2+}$and Ba^{2+} ions in solution using the following equation.

$$\boldsymbol{Percentage\ inhibition}\ (\%) = \frac{m_2 - m_0}{m_1 - m_0}\ X\ 100\%$$

where m_2 is the mass concentration of Ca^{2+} and Ba^{2+} ions after inhibitor functions, m_1 is the mass concentration of Ca^{2+} and Ba^{2+} ions in the solution of 50 mL deionized water without the addition of anions

solution, m_0 is the mass concentration of Ca^{2+} and Ba^{2+} ions of the solution with no inhibitor. The test of the mass concentration of Ca^{2+} and Ba^{2+} ions also followed the method specified by the standard, TM0374-2007.

Table 1: Static jar test conditions

Scale type	Brine	Concentration (g/L)	Condition
$CaSO_4$	cation anion	NaCl = **7**.50; $CaCl_2 \cdot 2H_2O$ = 11.10 NaCl = **7**.50; Na_2SO_4 = 10.66	70 ^oC & 90 ^oC 4 Hrs & 22 Hrs
$CaCO_3$	cation anion	$CaCl_2 \cdot 2H_2O$ = 12.15; $MgCl_2 \cdot 6H_2O$ = 3.68; NaCl = 33.0 $NaHCO_3$= 7.36; NaCl = 33.0	70 ^oC & 90 ^oC 4 Hrs & 22 Hrs
$BaSO_4$	cation anion	NaCl = 7.50, $BaCl_2 \cdot 2H_2O$ = 0.66 NaCl = 7.50, Na_2SO_4 = 0.80	70 ^oC & 90 ^oC 4 Hrs & 22 Hrs

3. Results and Discussion

3.1. Properties of ROSE and its Derivatives

Solubility of ROSE in aqueous medium and other parameters investigated are presented in Table 2. The pH measurement of the scale inhibitors, labelled ROSAC, ROS, were 8.5 and 8.0. This implies that the two products pass the criteria of a pH greater than five (>5). ROS was more soluble in water than ROSAC. This informed the decision to use ROS for further evaluation

Table 2: Properties of inhibitors

ROSE Derivatives	ID	Solubility in water	Colour	pH
ROSE Extracted with Acetone	ROSAC	Insoluble	Light Brown	8.5
ROSE Extracted with 1% NaOH in water	ROS	Soluble	Reddish Brown	8.0

3.2. Characterization of scale inhibitor

The FTIR spectra shown in Figure 2b was used to confirm the structure of the tested inhibitor (ROS). The peak value around 3257 cm^{-1} is attributed to the broad O-H stretching vibration for phenolic compounds. The aromatic C-H stretching vibrations are confirmed by peaks at 2918 cm^{-1} and 2851 cm^{-1}. The band at 1756 cm^{-1} is caused by the C=O stretching vibration, and the band at 1562 cm-1 is caused by the C=C and C=O

stretching vibrations of the gamma-pyrone in ring C of the quercetin structure. The peak at 1439 cm^{-1} results from C-H asymmetric deformation vibration, while the peak at 1410 cm^{-1} results from the O-H deformation vibrations and the C-O stretching vibration. Peaks 870 cm^{-1}, 803 cm^{-1} and 784 cm^{-1} are due to the C-H out of plane deformation vibrations of the isolated aromatic C-H hydrogen atoms in the quercetin structure.The wavelength around 1071 cm^{-1} confirms the C-O-C stretching vibration. These observations agree with those of other works [28, 3] and are consistent with the bonds that make up the major constituents (quercetin). The presence of quercetin and other important compounds supports the present study.

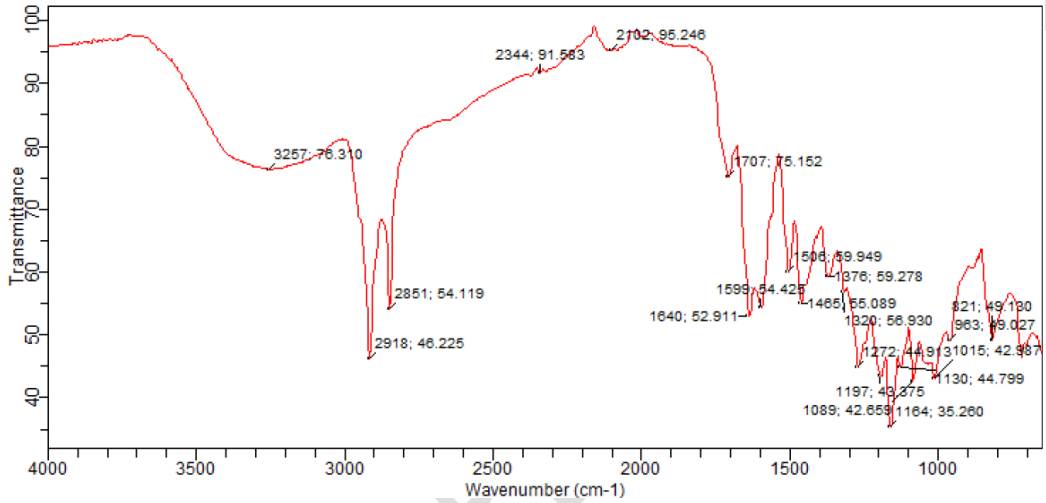

(a)

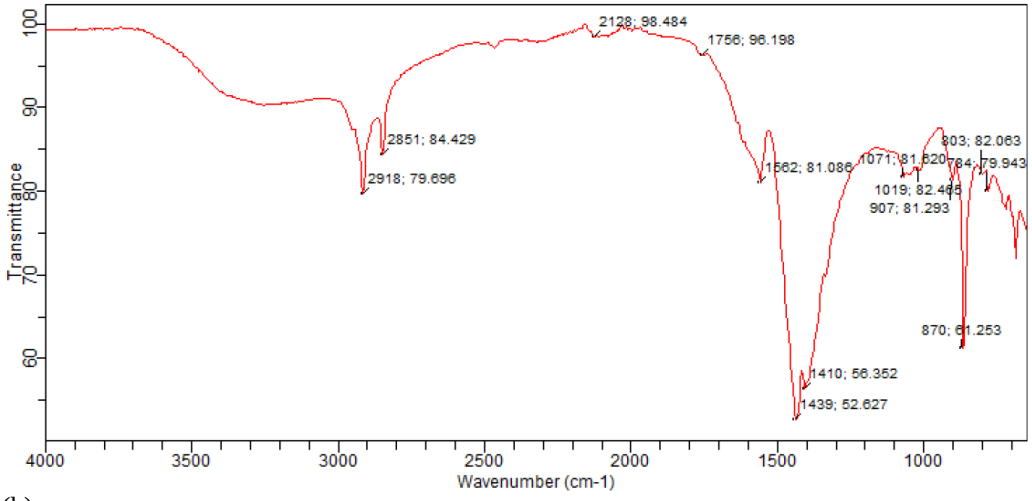

(b)

Figure 2: FTIR spectrum of (a) ROSAC and (b) ROS

3.3. Evaluation of scale inhibition performance

Figure 3 depicts the inhibitor's inhibition performance of calcium sulfate (Figure 3a), calcium carbonate (Figure 3b), and barium sulfate (Figure 4) with different inhibitor dosages at 71 ^{o}C. It was generally observed that increasing the inhibitor dosage increases the inhibitor's inhibition efficiency. When the dosage reaches a critical level, the inhibition rate remains constant or slowly decreases.

In the case of calcium sulfate (Figure 3a), the inhibitor demonstrated a good inhibition efficiency at a low dosage of 20 ppm, and the best inhibition efficiency of 70 % was obtained at a dosage of 80 ppm. The inhibition rate was low across all dosages in the calcium carbonate inhibition performance test (Figure 3b). Based on the scope of this work, an inhibition efficiency of only 50% was obtained at the optimum dosage of 100 ppm. However, barium sulphate inhibition evaluation provided the highest inhibition efficiency of 83 % at a dosage of 80 ppm before reaching a plateau state (Figure 4). As a result, ROS has a relatively good inhibition performance on both the calcium and barium sulfate scales. Figure 3,4,5 (b) shows a close relationship in the performance of ROS and a commercial scale inhibitor (CSI) evaluated at the same laboratory condition.

a) b)

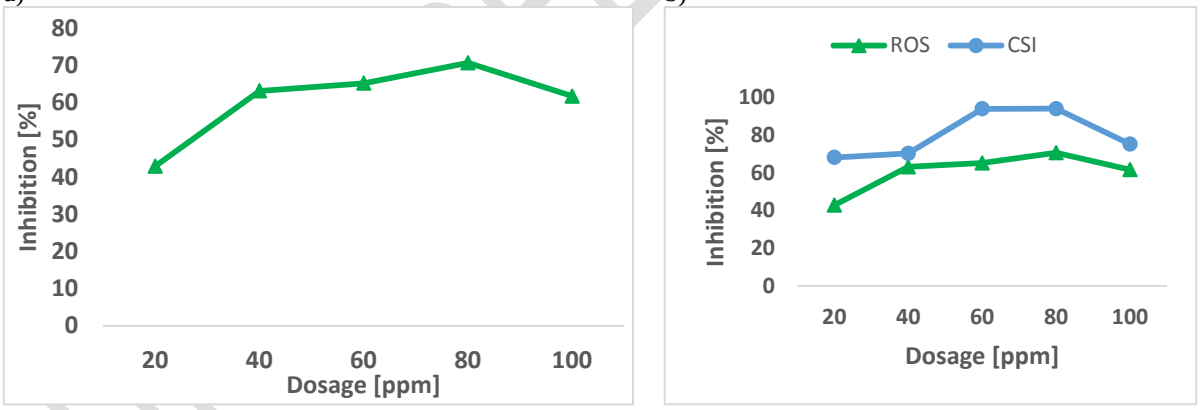

Figure 3: a) Relation curve of dosage to inhibition efficiency of ROS on calcium sulfate scale, (b) comparison of ROS and CSI performance on calcium sulphate scale

a) b)

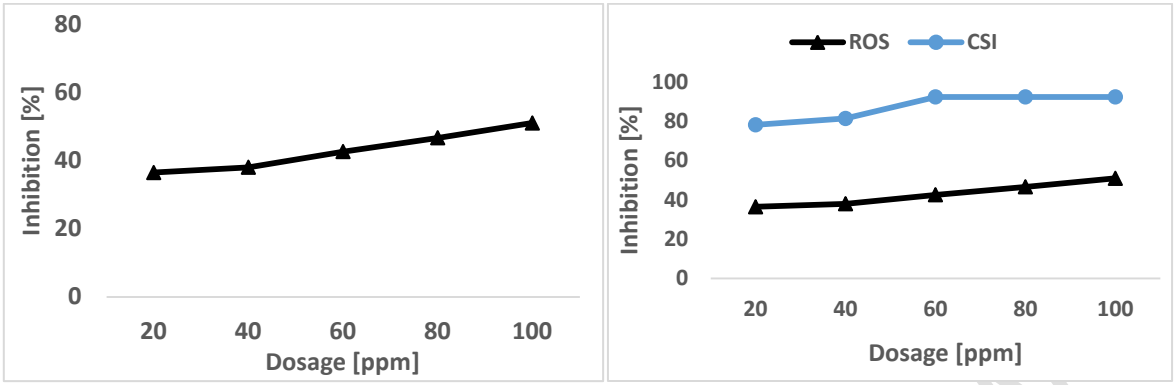

Figure 4: a) Relation curve of dosage to inhibition efficiency of ROS on calcium carbonate scale, (b) comparison of ROS and CSI performance on calcium carbonate scale.

a)

b)

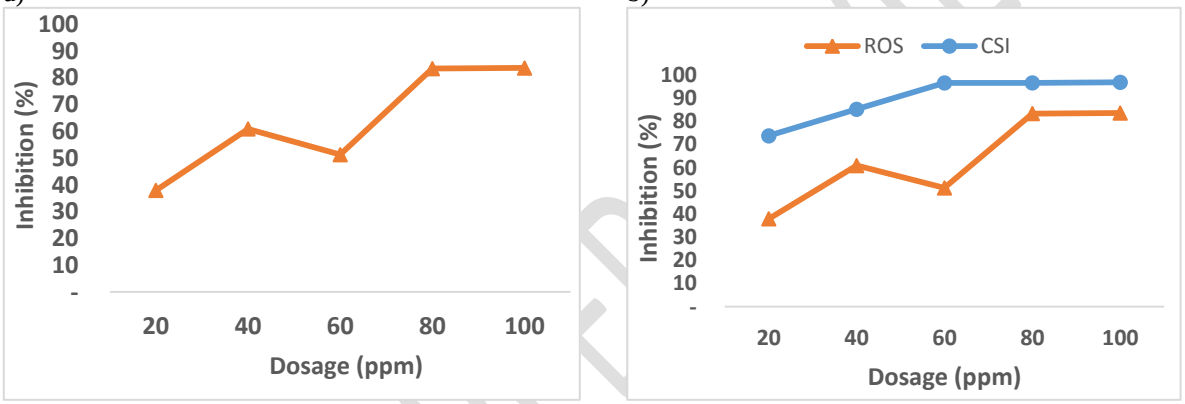

Figure 5: a) Relation curve of dosage to inhibition efficiency of ROS on barium sulfate scale, (b) comparison of ROS and CSI performance on barium sulphate scale

3.4 Effects of Temperature and Time on the inhibition performance of the antiscalant

3.4.1. Temperature

For inhibition property on calcium sulfate (Figure 5a), when a dosage of 60 ppm was added, an identical inhibition rate of 65 % was obtained at 71 ^{o}C and 90 ^{o}C. From Figure 5b, the scale inhibition efficiency on calcium carbonate is greater than 40% with a dosage of 20 ppm at 71 ^{o}C and nearly 60 ppm at 90 ^{o}C. This could be attributed to the fact that high temperatures facilitate the formation of calcium carbonate; as a result, an additional inhibitor dosage is required for improved efficiency. When the dosage is increased to a certain level (60 ppm), the inhibition rate at 90 ^{o}C is greater than at 71 ^{o}C, indicating that more inhibitor adsorption occurs on the calcium carbonate crystal at higher temperatures [29].

a)

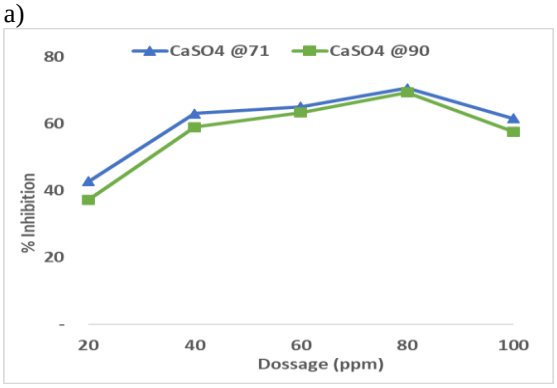

b)

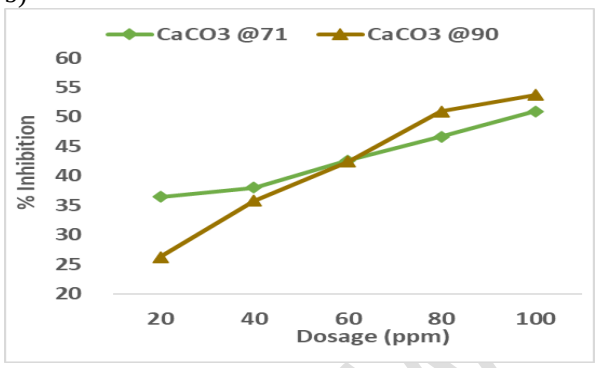

Figure 6: Effects of Temperature on the inhibition performance of ROS on (a) Calcium sulphate (b) calcium carbonate.

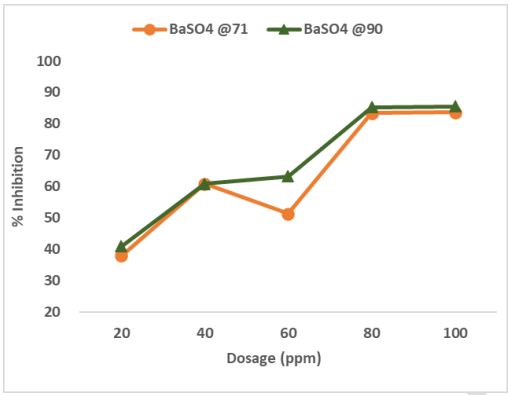

Figure 7: Effects of Temperature on the inhibition performance of ROS on barium sulphate

For barium sulfate (Figure 6), when the optimal dosage at 60 ppm was added, almost identical inhibition rate of about 60 % was obtained at both 71 ^{o}C and 90 ^{o}C. Therefore, it can be inferred that at higher temperatures, additional inhibitor dosage is required to maintain a high inhibition rate for $CaCO_3$ inhibition, whereas $BaSO_4$ control requires no additional dosage in the scope of this work.

3.4.2. Time

Effect of inhibition time on the performance of scale inhibitor is shown in Figure 7. For calcium sulphate deposition inhibition experiments (Figure 7a), the scale inhibition rate increases at a higher time duration. The inhibition efficiency on calcium carbonate is also increasing at a higher time duration (Figure 7b). At an evaluation time of 22 hrs, $CaCO_3$ has an inhibition rate of 50 % which is higher when compared to 39 % obtained for 4hrs inhibition time. This indicates that the inhibitor plays a continuous $CaSO_4$ and $CaCO_3$ inhibition performance.

a)

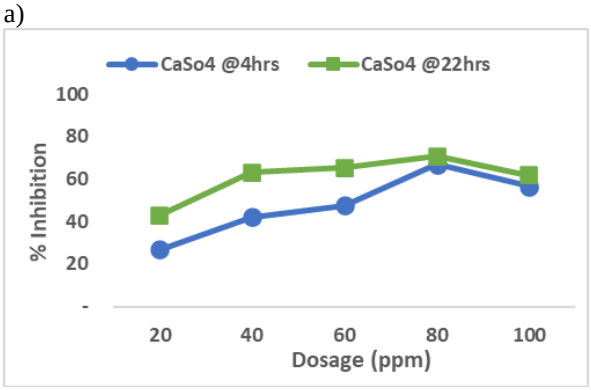

b)

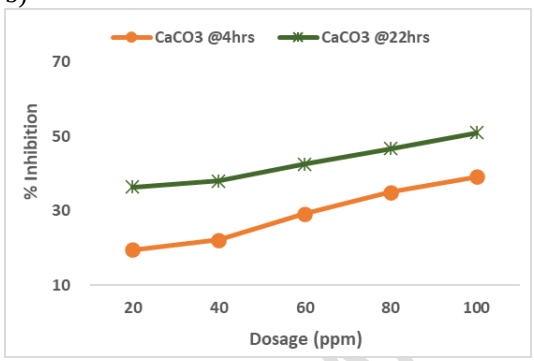

Figure 8: Effects of time on the inhibition performance of ROS on (a) Calcium sulphate (b) calcium carbonate, (c) barium sulphate

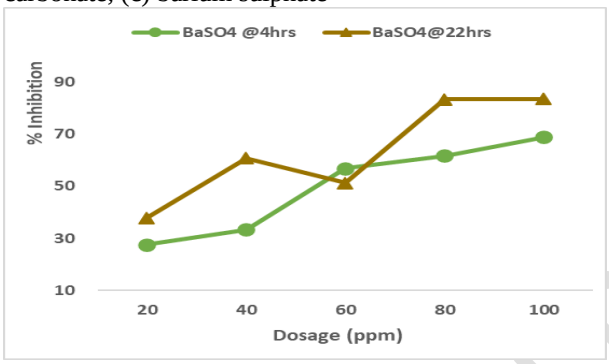

Figure 9: Effects of time on the inhibition performance of ROS on barium sulphate

For barium sulphate deposition (Figure 8), there was also an increase in inhibition efficiency for 22 hrs up until 60 ppm, before a sharp decrease in the inhibition rate and thereafter, a rise with increased dosage. This phenomenon suggests that a sufficient dosage for controlling barium sulfate scale deposition may be required in a long time.

3.5. SEM Analysis

SEM images of calcium sulphate, calcium carbonate, and barium sulfate, obtained from the absence and low dosage of inhibitor is shown in Figure 9, 10, 11 respectively. When an inhibitor was added to calcium carbonate crystals, they became looser (Figure 10c), an indication of crystal growth suppression. A similar phenomenon was observed for calcium sulfate (Figure 9c), where the dense structure changed to lose lump. Fluid turbulence could easily disrupt the loose material, causing it to become suspended in the solution [29-30]. Also, in the presence of the inhibitor, the diameter of the calcium carbonate and calcium sulfate crystals increases, indicating that the inhibitor may have some influence on the surface phase of these scales [31].

Figure 11 depicts a densely packed crystal of barium sulphate before conditioning and without inhibitor (Figure 11a). Figure 11c shows that the addition of the inhibitor resulted in lose particles. This demonstrates that the preferential growth of barium sulphate crystals was strongly inhibited.

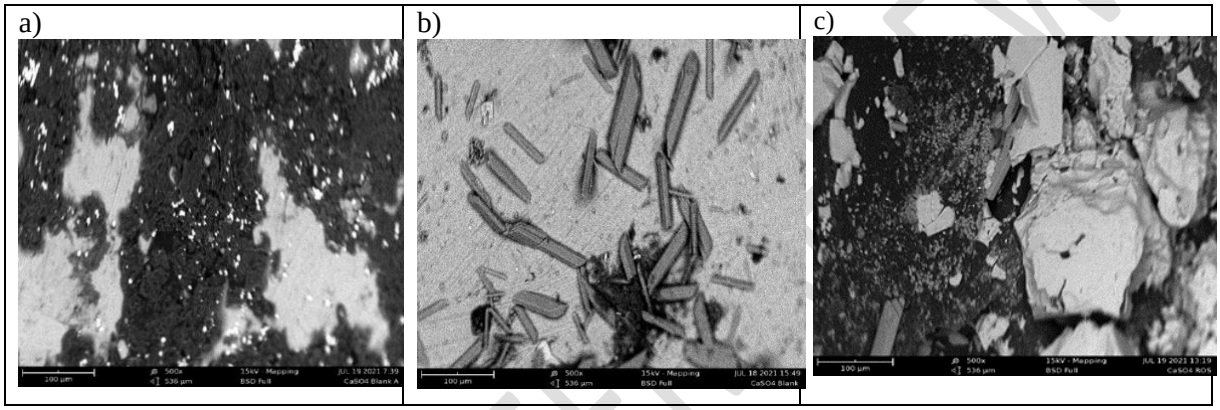

Figure 10: SEM images of $CaSO_4$ without inhibitor before and after conditioning (a, b) and with inhibitor (c)

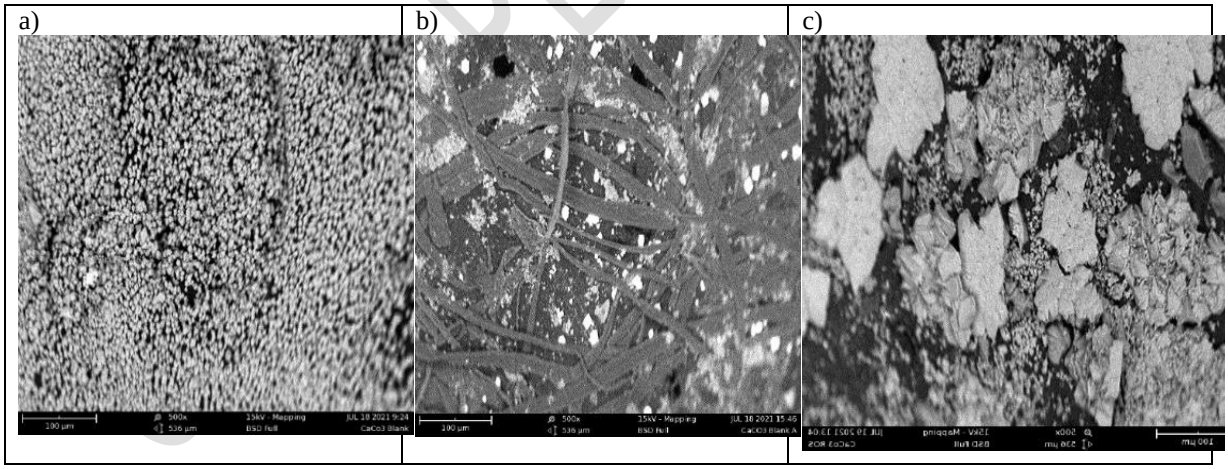

Figure 11: SEM images of $CaCO_3$ without inhibitor before and after conditioning (a, b) and with inhibitor (c)

a)	b)	c)

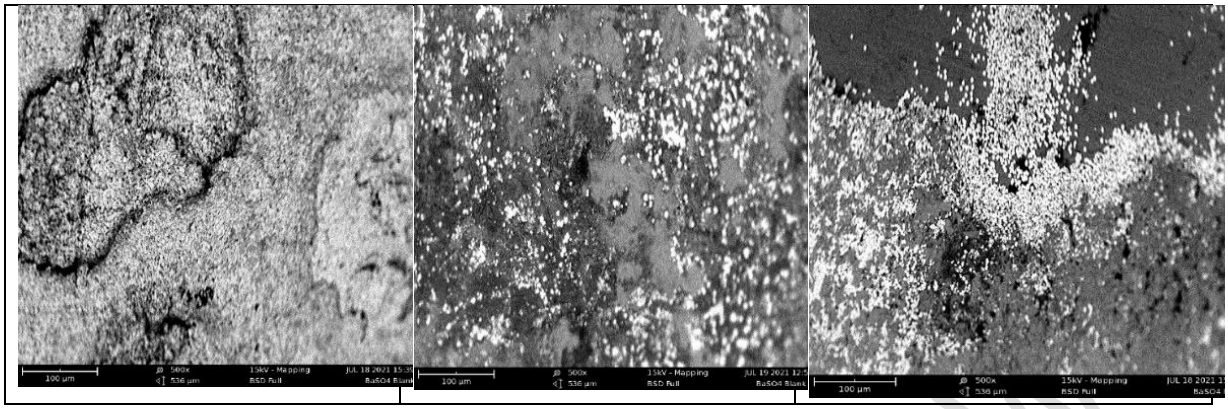

Figure 12: SEM images of $BaSO_4$ without inhibitor before and after conditioning (a, b) and with inhibitor (c)

4. Conclusions

1. A potential green scale inhibitor for oilfield is developed and evaluated on calcium sulfate, calcium carbonate, and barium sulfate scales. For calcium sulphate, the inhibition efficiency could be as high as 69 %, and for barium sulphate, it could be as high as 85%. Calcium carbonate had a lower inhibition rate than the other scales evaluated. The highest inhibition rate of 53% was obtained at a dosage of 100 ppm.
2. The developed inhibitor has good chemical stability, high-temperature resistance, and good scale inhibition effects at low dosage.
3. Extra inhibitor is required for good inhibition of calcium carbonate deposition at higher temperatures, but it is not required for calcium sulphate and barium sulfate scale inhibition.
4. Because the diameter of calcium sulfate and calcium carbonate formed when inhibitor is present is larger than that formed at blank conditions, proper dosage is critical for calcium sulfate and calcium carbonate prevention.
5. Comparison with an existing commercial inhibitor (CSI) show that ROS has a good potential as green scale inhibitor in the oil industry.

COMPETING INTERESTS DISCLAIMER:

Authors have declared that no competing interests exist. The products used for this research are commonly and predominantly use products in our area of research and country. There is absolutely no conflict of interest between the authors and producers of the products because we do not intend to use these products as an avenue for any litigation but for the advancement of knowledge. Also, the research was not funded by the producing company rather it was funded by personal efforts of the authors.

References

1. JI Al-Tammar, M Bonis, HJ Choi and Y Salim. Saudi Aramco downhole corrosion/scaling operational experience and challenges in HPHT gas condensate producers. *SPE international oilfield corrosion conference and exhibition*. Aberdeen, Scotland, 2014.
2. R Hosny, M Amine, M Fathy and M Ramzi M. Investigation of the Impact of Scale Inhibitors: Nonionic Surfactants for Scale Deposition Control in Oilfield. *Pet Petro Chem Eng Journal*. 2019; 3(2), 189.
3. G. Manizabayo, UJ Chukwu and OJ Abayeh. Extraction of "Quercetin-Rich" Red Onion Skin with Acetone and Chemical Modification using Aromatic Diazonium Salts. *Makara Journal of Science*. 2019; 23 (2) 3.
4. T Chen, A Neville and M Yuan. Calcium carbonate scale formation-assessing the initial stages of precipitation and deposition. *J Pet Sci Eng.* 2005; 46(3),185- 194.
5. MCM Bezerra, FF Rosario and KRSA Rosa. Scale management in deep and ultradeep water fields. *Offshore Technology Conference*, Brazil. 2013
6. R Hosny, SEM Desouky, M Ramzi, TH Abdel-Moghny and FMS El-Dars. Novel scalechem program for monitoring and enhancing dissolution of scale deposits near wellbore. *Material Science Research India.* 2007; 4(2), 251-261.
7. R Hosny, SEM Desouky, M Ramzi, TH Abdel-Moghny and FMS El-Dars. Estimation of the Scale Deposits Near Wellbore via Software in the Presence of Inhibitors. *Journal of Dispersion Science and Technology.* 2009; 30(2), 204-212.
8. MA Awan and SM Al-Khaledi. Chemical treatments practices and philosophies in oilfields. *SPE international oilfield corrosion conference and exhibition*, Aberdeen, Scotland, 2014.
9. D Hasson, H Shemer and A Sher, A. State of the art of friendly "green" scale control inhibitors: a review article. *Ind. Eng. Chem. Res*. 2011; 50, 7601 – 7607.
10. M Chaussemier, E. Pourmohtasham, D Gelus, N Pécoul, H Perrot, J Lédion, H Cheap-Charpentier and O Horner. State of art of natural inhibitors of calcium carbonate scaling. Desalination. 2015; 356, 47-55.
11. PT Anastas and JC Warner. Green Chemistry: Theory and Practice, vol.11, *Oxford University Press*, New York, 1998, p 13-43.
12. R Aidoud, A Kahoul and F Naamoune. Inhibition of calcium carbonate deposition on stainless steel using olive leaf extract as a green inhibitor. *Environmental Technology Journal*. 2017: 38, 14-22.
13. NS Alrawaiq and A Abdullah. A Review of Flavonoid Quercetin: Metabolism, Bioactivity and Antioxidant Properties. *Int. J. PharmTech Res*. 2014; 6(3): 933–941.

14. G Dehghan and Z Khoshkam. Chelation of Toxic Tin (II) by Quercetin: A Spectroscopic Study. Int. Conf. Life Sci. Technol. 2011; 3, 3–5.
15. P Lakhanpal and DK Rai. Quercetin: A Versatile Flavonoid. *Internet J. Med. Update.* 2007; 2(2): 22–37, https://doi.org/10.4314/ijmu.v2i2.39851.
16. Y Liu and M Guo. Studies on Transition Metal- Quercetin Complexes Using Electrospray Ionization Tandem Mass Spectrometry. Molecules. 2015; 20, 8583–8594. https://doi.org/10.3390/molecules20058583
17. M Symonowicz and M Kolanek. Flavonoids and their properties to form chelate complexes. *Biotechnol. Food Sci*. 2012; 76(1): 1-7.
18. FB Mohd, A Razak, PK Yong, LC Abdullah, SS Yee and TC Yaw. The effects of Varying Solvent Polarity on Extraction Yield of Orthosiphon Stamineus Leaves. *J. Appl. Sci*. 2012; 12(11), 1207–1210, https://doi.org/10.3923/jas.2012.120 7.1210
19. M Horbowicz. Method of quercetin extraction from dry scales of onion. *Veget.Crops Res. Bull*. 2002; 57, 119-124.
20. HS Sayed, NMM Hassan and MHA El. The Effect of Using Onion Skin Powder as a Source of Dietary Fiber and Antioxidants on Properties of Dried and Fried Noodles. *Current Sci. J*. 2014; 3(4), 468–475.
21. BOT Ifesan. Chemical Composition of Onion Peel (Allium cepa) and its Ability to Serve as a Preservative in Cooked Beef. *Int. J. Sci. Res. Methodol*. 2017; 7(4), 1-10.
22. MO Bello, IO Olabanji, M Abdul-Hammed and TD Okunade. Characterization of domestic onion wastes and bulb (Allium cepa L.): fatty acids and metal contents. *Int. Food Res. J*. 2013; 20(5): 2153– 2158.
23. AA Akaho, UJ Chukwu and O Akaranta. Cu (II)-Red Onion Skin Extract-Azo metal Complex - A Potential for Oilfield. *Chemical Science International Journal*. 2019; 24-56
24. SE Itodo, S Oyero, EU Umeh, A Ben and MD Etubi. Phytochemical Properties and Staining Ability of Red Onion (Allium cepa) Extract on Histological Sections. *J Cytol Histol.* 2014; 5:275. doi:10.4172/2157-7099.1000275
25. HN Dike, A Dosunmu, O Akaranta and B Kinigoma. Effect of Cashew Nut Shell Liquid Esters on KCL/Polymer/Glycol Drilling Fluid Flow Property. *International Journal of Technical & Scientific Research Engineering*. 2019; 2, 2581-9259.
26. NACE Standard TM0197-2010, Item No. 21228, Laboratory Screening Test to Determine the Ability of Scale Inhibitors to Prevent the Precipitation of Barium Sulfate or Strontium Sulfate, or Both, from Solution (for Oil and Gas Production Systems)
27. NACE Standard TM0374-2007 (formerly TM0374-2001) Item No. 21208, Laboratory Screening Tests to Determine the Ability of Scale Inhibitors to Prevent the Precipitation of Calcium Sulfate and Calcium Carbonate from Solution (for Oil and Gas Production Systems)
28. M Heneczkowski, M Kopacz, D Nowak and A Kuźniar. Infrared spectrum analysis of some flavonoids. *Acta Pol Pharm*. 2001; 58, 415-20
29. H Luo, D Chen, X Yang, X Zhao, H Feng, M Li and J Wang. Synthesis and performance of a polymeric scale inhibitor for oilfield application. *J Petrol Explor Prod Technol*. 2015; 5:177–187
30. ZH Shen, JS Li, K Xu, LL Ding and HQ Ren. The effect of synthesized hydrolyzed polymaleic anhydride (HPMA) on the crystal of calcium carbonate. *Desalination* 2012; 284, 238–244.
31. E Mavredaki, A Neville, KS Sorbie. Initial Stages of Barium Sulfate Formation at Surfaces in the Presence of Inhibitors. *Cryst Growth Des* 2011; 11, 4751–4758